



UNIVERSITY OF LEEDS

This is a repository copy of *Graphite nanoplatelet/rubbery epoxy composites as adhesives and pads for thermal interface applications*.

White Rose Research Online URL for this paper:
<http://eprints.whiterose.ac.uk/128611/>

Version: Accepted Version

Article:

Raza, MA, Westwood, A orcid.org/0000-0002-5815-0429 and Stirling, C (2018) Graphite nanoplatelet/rubbery epoxy composites as adhesives and pads for thermal interface applications. *Journal of Materials Science: Materials in Electronics*, 29 (10). pp. 8822-8837. ISSN 0957-4522

<https://doi.org/10.1007/s10854-018-8900-z>

Reuse

Items deposited in White Rose Research Online are protected by copyright, with all rights reserved unless indicated otherwise. They may be downloaded and/or printed for private study, or other acts as permitted by national copyright laws. The publisher or other rights holders may allow further reproduction and re-use of the full text version. This is indicated by the licence information on the White Rose Research Online record for the item.

Takedown

If you consider content in White Rose Research Online to be in breach of UK law, please notify us by emailing eprints@whiterose.ac.uk including the URL of the record and the reason for the withdrawal request.



eprints@whiterose.ac.uk
<https://eprints.whiterose.ac.uk/>

**Graphite nanoplatelet/rubbery epoxy composites as adhesives and pads for
thermal interface applications**

Mohsin Ali Raza^{*1}, Aidan Westwood², Chris Stirling³

¹Department of Metallurgy and Materials Engineering, College of Engineering and Emerging
Technologies, University of the Punjab, Lahore, Pakistan

²School of Chemical and Process Engineering, University of Leeds, LS2 9JT, UK

³Morgan Advanced Materials, Swansea, SA6 8PP, UK (current address: Haydale Ltd.,
Ammanford, SA18 3BL, UK)

Submitted to

Journal of Materials Science: Materials in Electronics

Nov. 2017

*Corresponding author Email: mohsin.ceet@pu.edu.pk (Mohsin Ali Raza)

Tel: +92 334 4007940

Abstract

Composites of graphite nanoplatelets (GNPs) and rubbery epoxy (RE) resins as adhesives and pads are evaluated as thermal interface materials (TIM). GNP-15 and GNP-5 (15 μm and 5 μm across, respectively) were loaded in RE by 3-roll milling to produce GNP/RE composites. The role of composite processing techniques on the texture, thermal and electrical conductivities and compression properties of composites was studied and compared. Scanning electron microscopy revealed uniform dispersion of GNPs in RE, regardless of loading and x-ray diffraction texture measurement showed less platelet alignment in the composites at low loadings. Thermal conductivities of 20 wt. % GNP-15/RE (3.29 W/mK) and 35 wt. % GNP-5/RE composite (2.36 W/m.K) were both significantly higher than pure RE (0.17 W/m.K). GNP/RE retained good compliance, compressive moduli at 20 wt. % loading being comparable to commercial BN/silicone TIM. Although thermal contact resistance of GNP/RE was higher than for commercial paste, its interfacial thermal transport outperformed GNP/silicone (due to RE's strongly adhesive nature) and, across thick bond lines, outperformed reported GNP-pastes. The 20 wt. % GNP-15/RE thermal pad had significantly lower thermal contact resistance than other GNP/RE pads. This decreased with increasing applied pressure, being comparable to commercial BN/silicone pad. GNP/RE composites are thus promising candidates for thermal interface adhesives and pads.

1. Introduction

The ever-decreasing size of microelectronic devices has resulted in higher power densities in much smaller spaces, leading to high heat evolution from the devices, which if not effectively removed would result in reductions in performance (e.g. switching delays) and reliability (e.g. thermally stressed, and then cracked, solder joints). Thermal management strategies are thus essential for electronics cooling and key to this are thermal interface materials (TIMs) [1-3]. Commercially, TIMs are employed in the form of heat dissipation compounds which primarily consists of polymer matrix/carrier in which thermally conducting fillers such as silver, aluminum nitride, boron nitride or SiC are dispersed at loadings of 50-70 wt.%. Such polymer matrix compounds can be used as the thermal grease/paste or adhesives [4, 5]. These TIMs reduce interfacial thermal contact resistance between mating surfaces and thus facilitate heat dissipation. Both thermal grease/paste or adhesive are mainly employed for thin gap filling applications [4, 6]. However, when gap between mating surfaces is significantly large TIMs in the form of thermal pads are used [7]. Thermal pads are similar to thermal adhesives but the polymer matrix is very compliant in nature such as silicone.

The thermal transport ability of TIMs strongly depends on the thermal conductivity of filler [8]. Carbon nanomaterials such as graphene, graphite nanoplatelets and carbon nanofibres have significantly higher thermal conductivity (>1000 W/m.K) [9, 10] than other inorganic fillers (BN, AlN or SiC) and therefore these have been extensively researched for development of next-generation polymer-based TIMs [11-14]. A graphite nanoplatelet (GNP) is a 2-dimensional nanomaterial which can have thickness of 10-100 nm [15] and lateral width of several microns. Since it comprises of multilayer graphene sheets, it could offer comparable thermal conductivities in TIMs to that of graphene. However, unlike graphene, GNPs are cheap fillers which can be produced easily in high quantities.

GNP-based epoxy and silicone composites have been reported for thermal interface applications on the basis of their high thermal conductivities [11, 16]. The thermal contact resistance between a

semiconductor die and a heat sink or spreader is a major hindrance in the dissipation of heat from the die to heat sink [8] but this has not been evaluated much for GNP-based TIMs. The present study reports GNP/rubbery epoxy composites produced by three-roll milling (RM) and quantifies their heat dissipating ability as thermal interface adhesives and thermal pads by measurement of thermal contact resistance according to ASTM D5470, which to some extent replicates conditions in which electronic devices operate [10]. The properties of the composites produced by RM are compared with the similar composites produced by mechanical mixing (MM) and speed mixing (SM) previously reported by us [17].

2. Experimental

GNPs (EX. XG Sciences) of sizes 5 μm (GNP-5) and 15 μm (GNP-15) [17] were dispersed at a loading of 8-35 wt. % in a rubbery epoxy (RE) [18] resin using three RM (model 80E from EXAKT GmbH). The same protocol was followed for the production of composites as was reported in [19]. The composites were also fabricated as thermal pads/sheets by curing the dispersions (120 °C for 3 h) in a custom-made mould under a pressure of 0.3 MPa. The freeze-fractured and Pd/Pt alloy sputter coated-samples were examined by scanning electron microscopy (FEG-SEM, LEO/Zeiss, Gemini 1530 field) to determine dispersion quality of GNPs in RE resin. The thermal conductivity and compression properties of composites were measured using a hot disk thermal analyser (Hot Disk AB) and a universal testing machine (Instron Model no. 3382 with a 100 kN load cell), respectively. The diffraction patterns were acquired by a Philips PW3040/60 diffractometer (Cu- K_{α} , 40 kV, 40 mA, 10-90° 2 θ , 0.02° step, 20 s step⁻¹) of as-received GNPs and the GNP/RE composites according to the method described in [20]. The X-ray texture scans were obtained in a Philips texture goniometer (PW2030) using Cu K_{α} radiation with a Schulz reflection-specimen holder following the method described in [19]. The electrical conductivity was measured on the cuboidal-shaped samples using two-probe method. Electrical conductivity was measured through the sample in the direction parallel to the direction of gravity during curing (σ_{\parallel}) and perpendicular

to it, i.e., along the roll milling direction (σ_{\perp}). For thermal contact resistance measurement, composite dispersions were sandwiched (in uncured form) between copper cylinders and tested in a thermal contact resistance measurement rig in uncured form or cured in-situ according to the procedure described in [21, 22]. The thermal contact resistance of thermal pads was measured in the same rig by sandwiching pads between copper cylinders.

3. Results and discussion

3.1 Loadings of GNPs into RE

GNP-15 and GNP-5 can be loaded into the RE matrix at maximum loadings (to retain workability) of 25 and 35 wt. %, respectively by RM technique. Similar level of loadings were produced previously by MM and SM techniques [17]. It was noted that GNP-15s can be loaded at higher than 25 wt. % by the three RM process but the resulting composite had highly crumbly nature because there was not enough resin to wet the surface of the GNPs due to their high surface area and aspect ratio. GNP-5 particles can be loaded up to 35 wt. % by RM without losing workability.

3.2 Viscosity of GNP/RE dispersions

Plots of viscosity versus shear rate for pure RE and GNP/epoxy dispersions produced by RM are presented in Fig. 1. For comparison viscosities of dispersion produced by MM are also presented in Fig. 1.

Fig. 1

At the start of the test, shear rate was low and viscosity was high (Fig. 1). However, with a small increase of shear rate of about 10-15 s^{-1} , the viscosities dropped rapidly and then leveled off. The viscosity of pure RE resin is about 600 cP at a shear rate of 15 s^{-1} . The GNPs dispersed in either RE or glassy epoxy by MM increased the viscosity of the dispersions at 20 wt. % loading. The viscosities of the 20 wt. % GNP-5/RE dispersion and 20 wt. %

GNP-15/RE dispersion at a shear rate of 15 s^{-1} are about 1,400 and 16,300 cP, respectively. The higher viscosity of the 20 wt. % GNP-15/RE dispersion is presumably due to the large particle size of the GNP-15s compared to that of the GNP-5s. Large particles can reduce the free volume in the epoxy matrix and also undergo strong interaction with each other resulting in an increased viscosity of the epoxy dispersion. Unlike the composite dispersions produced by MM, the dispersions of GNP-15/RE produced by RM at 15 and 20 wt. % loading of GNP-15s had significantly higher viscosity. For instance, the viscosity of the GNP-15/RE composite dispersion produced by RM at 20 wt. % GNP-15 loadings is $\sim 432,500 \text{ cP}$ at a shear rate of $\sim 15 \text{ s}^{-1}$. This is $\sim 100\times$ higher than the equivalent dispersion produced by MM. The significantly higher viscosity of the GNP-15/RE composite dispersion indicates that the RM has produced greater dispersion of GNPs than that of the MM. Greater dispersion means that fewer GNPs agglomerate and more GNPs are available to adsorb the polymer on their surface and to interact with one another. Ganguli et al. [23] reported the viscosity of a 20 wt. % exfoliated graphite/glassy epoxy dispersion; this is about ten times higher than 20 wt. % GNP-15/RE dispersion produced by RM. This shows that RE dispersion is more workable compared to glassy epoxy dispersions.

3.3 SEM of GNP/RE composites produced by RM

SEM images of composites produced by RM at 8-25 wt. % loading of GNP-15 are presented in Fig. 2. SEM image of 25 wt. % GNP-5/RE composite produced by RM is also presented in Fig. 2. A summary of dispersion quality and morphology of GNP/epoxy composites produced by RM and their comparison with previously developed similar composites produced by MM and SM are presented in Table 1.

Fig. 2

RM produced GNP/RE composites with greater dispersion of GNPs. SEM images of GNP/RE composites (Fig. 2) at a loading of 8-20 wt. % GNPs are very similar and are completely

dominated by GNPs. It is very difficult to identify matrix in these images which demonstrates a much better dispersion of GNPs. Most of the GNPs are touching each other and form interconnects with each other to develop conducting networks. Even the composites produced at 8 wt. % and 15 wt. % loading (Fig. 2 (a-d)) have interconnected GNPs and this shows that the RM is capable of producing greater dispersion even at low loadings.

The composite produced with GNP-5 particles at 25 wt. % loading (Fig. 2 (i & j)) also has well dispersed and interconnected GNPs. Although, it was observed that 20 wt. % GNP-15/RE dispersion produced by RM has 10× higher viscosity than 20 wt. % GNP-15/glassy epoxy [17], no voids were observed in the roll milled sample (Fig. 2(e & f)).

The interesting feature of the RM is that it enables production of a composite with homogeneous distribution of GNPs at low loadings. In contrast, both MM and SM previously reported in [17] were unable to produce composites with uniform distribution of GNPs at low loadings. Fig. 2 (a) clearly shows that composites produced by RM have no concentration gradient of GNPs at 8 wt. % loading unlike the composites reported before in [17]. It appears that both MM and SM could not break agglomerates of the GNPs at low viscosities of the dispersions. Agglomerated-GNPs easily settled in the low viscosity RE resin during the 5 h of curing leading to a high concentration gradient in 10 mm thick as-cast samples of composites produced at low loadings. The SEM analysis clearly shows that the RM is superior over other processing techniques in developing composites with greater dispersion at low and high loadings.

3.4 Effect of processing on the thickness of GNPs

XRD patterns of the as-received GNPs (both GNP-15 and GNP-5) and the composites produced by the various processing techniques are presented in Fig. 3. The mean thicknesses of the as-received and processed GNPs can be measured from the broadening of the (0002) peaks and these are presented in Table 2.

Fig. 3

All GNP-15/RE composites produced by any technique have average thicknesses of GNP-15 ca. 35 nm (Table 2 and Fig. 3). It can also be observed that the GNP-5 thickness decreased to a similar value in the case of 25 wt. % GNP-5/RE composites produced by either MM or RM. This result shows that dispersion of GNPs in RE reduces thickness to some extent but further processing, e.g., increasing number of passes through rolls, increasing speed of mixing or time, could not produce thinning of GNPs.

3.5 Texture of GNP/RE composites produced by the RM

XRD pole figures of GNP-15/RE composites produced by the RM are presented in Fig. 4. The composites produced at 8 and 15 wt. % of GNP-15 loadings are not strongly textured because a significant fraction of 0002 plane normals are not oriented about the settling plane normal ($\psi = 15-60^\circ$) (Fig. 4 (a & b)). On the other hand, composites consisting of 20 and 25 wt. % GNP-15 platelets are strongly textured with a preferred [0002] normal to the settling plane (Fig. 4 (c & d)) with a bigger fraction of 0002 planes oriented at ($\psi = 15^\circ$) about the settling plane normal and in the direction of rolling. The composites produced at 35 and 60 wt. % GNP-15 platelets have the same preferred texture but with all 0002 planes oriented at ($\psi = 0^\circ$) the settling plane normal (Fig. 4 (e & f)). The texture analysis shows that the RM propensity to produce highly oriented GNP-composites increases with increasing GNP-15 loadings. Composites produced with GNP-5s are less textured compared to equivalent composites produced with GNP-15s (Fig. 4(g)). This suggests that the smaller GNP-5s produced more hindrance to the settling process. It was also observed that the 20 wt. % GNP-15/RE composite produced by RM developed strong texture when it was cured under pressure (Fig. 4(h)).

Fig. 4.

The effect of number of passes (i.e., dispersion passed through RM) on the texture in the RM processing is also investigated and is presented in Fig. 5. The 20 wt. % GNP-15/RE dispersion was passed through the RM 5, 10 and 15 times to produce composites. It can be seen from Fig. 5 that composites become more textured after 15 passes.

Fig. 5.

3.6 Effect of processing techniques on the texture of GNP/RE composites

A comparison of pole figures of 20 wt. % GNP-15/RE composites produced by the SM, MM and RM is presented in Fig. 6 (a-c). The 20 wt. % GNP-15/RE composites produced by RM and MM have similar texture i.e., GNP-15s are oriented at ($\psi = 0-30^\circ$) about the settling plane normal. On the other hand, equivalent composite produced by SM is less textured (Fig. 6 (b)). The 25 wt. % GNP-5/RE composite produced by MM has a bigger fraction of 0002 planes oriented at $\psi = 30-60^\circ$ resulting in a less oriented composite compared to an equivalent composite produced by RM (Fig. 6 (e)). This again suggests that smaller particles produce more hindrance to the alignment of GNPs in the composite at higher loadings. The samples of 20 wt. % GNP-15/RE and 25 wt. % GNP-5/RE composite produced by MM also achieved high texture when cured under pressure as shown in Fig. 6 (d & f), respectively.

Fig. 6

The texture measurements highlight that the RM produced increasingly highly textured composites at loadings of GNP-15 \geq 20 wt.%. The GNP-5s form less oriented composites at 25 wt. % loadings presumably because smaller particles form more hindrance to the alignment. It was found that both GNP-5s and GNP-15s reach a high degree of texture in a composite when the composite is cured under compression. Thus it is difficult to avoid GNP alignment/texture in these composites when they are produced for example as thermal pads by compression moulding.

3.7 Thermal conductivity of GNP/RE composites

Plots of the thermal conductivity of GNP-5/RE and GNP-15/RE composites (measured in a direction parallel to that in which gravity acted during curing in the mould) produced by RM are presented in Fig 7. For comparison thermal conductivity of similar composites produced previously by MM and SM processes as a function of wt. % of GNPs are also presented [17]. The values of thermal conductivity of the developed composites and pure epoxy are presented in Table 3.

Fig. 7

It can be observed from Fig. 7 and Table 3 that the thermal conductivity of the GNP/RE composites increases with the increase of both the wt. % of GNPs and the particle size of GNPs. The thermal conductivity of pure RE is 0.176 W/m.K and the thermal conductivity of the composites is higher than this at all wt. % loadings of the GNPs but there exists a very large data range in the thermal conductivity of the composites produced by MM and SM at GNPs loading ≤ 15 wt. % as shown in Fig. 7. In contrast, the data ranges in the case of composites produced by RM are negligible. The large data ranges in the case of composites produced by MM and SM resulted due to the presence of concentration gradients of GNPs as observed by SEM analysis [17]. Lower thermal conductivities were therefore measured when the sensor was sandwiched between upper cross-sections of the as-cast sample compared to when the sensor was sandwiched between lower cross-sections (high concentration region) of the as-cast sample. The absence of a concentration gradient in the composites produced by RM at 8 wt. % loadings clearly suggests that the RM produced composite (Fig. 2(a)) with greater dispersion than MM and SM. The greater dispersion of GNPs in the RM resulted in higher viscosities of dispersion as mentioned before and also more GNPs per unit volume (fewer agglomerates) which provided mutual hindrance to the settling in the resin. The thermal conductivity data show that the GNP/RE composites with a homogeneous thermal conductivity (without concentration gradient) can only be produced with MM and SM (under the

conditions studied in the previous work [17] at wt. % higher than 15 in the case of GNP-15 and at wt. % higher than 20 in the case of GNP-5 particles, since at these, and higher, loadings the content of GNPs is enough to overcome the settling, presumably because the filler particles hinder each other's movement under gravity.

The composites with greatest thermal conductivities at all loadings and in the case of both GNP-5s and GNP-15s were produced by RM. This result clearly demonstrates that RM produces composite with superior dispersion quality which resulted in many interconnects between GNPs in the matrix leading to the formation of highly effective conductive networks. The thermal conductivity of GNP-15/RE composites produced by RM at 20 wt. % loading increases ~19-fold to 3.29 W/m.K compared to the pure RE (0.176 W/m.K). This is ~2 times higher than the equivalent composites produced by MM and SM [17].

The thermal conductivity of GNP-5/RE composites produced by RM at 25 wt. % loading increases 8-fold to 1.47 W/m.K compared to the pure RE. The equivalent composite produced with large platelets (GNP-15) at 25 wt. % loading by RM has ~2 times higher thermal conductivity. The composite produced with large platelets (GNP-15s) at 20 wt. % loading has still ~1.5 times higher thermal conductivity than a composite produced with smaller platelets (GNP-5s) even at 35 wt. % loading by RM (2.36 W/m.K). These results show that the particle size of GNPs plays a vital role in the thermal transport behavior of the resulting composites. It is clear that at equivalent wt. % loadings, the thermal transport in composites with large particles is more effective than with small particles. In the case of large particles, fewer particles are involved in the formation of the conducting networks and hence there is reduced thermal contact resistance between the particles due to fewer interfaces.

The composites produced by RM at 8 and 15 wt. % loadings have thermal conductivities of 1.13 and 1.75 W/m.K, respectively (Table 3). On the other hand, the thermal conductivity of 20 wt. % GNP-15/RE composite is 1.4× higher than the equivalent silicone composite produced by RM

reported in [19]. This significantly high thermal conductivity of the RE composite, in this case, might be due to much thinner GNP-15s. On the other hand, the thermal conductivity of GNP-15/RE composite produced by RM at 25 wt. % loading is almost similar to that of the composite produced at 20 wt. % loading. The observed no increase in the thermal conductivity of 25 wt. % GNP-15/RE composite is perhaps an effect of much higher orientation of GNP-15s in this composite than that in 20 wt. % GNP-15/RE composite (Fig. 4 (c & d)) and this is also observed by electrical conductivity measurements as discussed in Section 3.9.

3.8 Comparison of thermal conductivities of GNP/RE composites with literature

Ganguli et al. [23] reported a thermal conductivity of 4 W/m.K for 20 wt. % exfoliated graphite/epoxy composite produced by SM which represents a 19-fold increase compared to the pure resin. The exfoliated graphite used had lateral dimensions of 4 μm and thickness of 100 nm while the minimum particle size of the GNPs used in the present study was 5 μm and thicknesses in the composites in the range of 30 nm. The thermal conductivity for 20 wt. % GNP-5/RE composite produced by SM was 5 times lower than that of Ganguli's 20 wt. % exfoliated graphite/epoxy composite [23]. The composite preparation method is almost identical to that of Ganguli et al. [23] but despite this the GNP/RE composites with slightly larger particle size (GNP-5), even at 30 wt.%, were unable to give the 19-fold improvement. Debalak et al. [24] reported the thermal conductivity of exfoliated graphite/epoxy composites for various particle sizes of exfoliated graphite. The highest value of thermal conductivity in their work (4.3 W/m.K) was achieved at 20 wt. % loading for all different sizes (50-150 mesh) of exfoliated graphite in the epoxy. Debalak et al.'s finding [24] that the thermal conductivity of exfoliated graphite/epoxy composites increased with the increase of the filler content corresponds well to the thermal conductivity data reported for the various particle sizes of GNPs in the present study. However, they found that the thermal conductivity values for all sizes of exfoliated graphite were almost the same at 20 wt. % loading. In

contrast, in the present work clear difference between the thermal conductivities of the composites produced with small and large particles even at high loadings was observed.

The nature and process of exfoliation of graphite used to produce GNPs can also influence the thermal conductivity of the GNP/epoxy composite. One main difference between this work and that of Ganguli et al. [23] and Debalak et al. [24] is the thermal conductivity measurement technique. In the present work, the thermal conductivities were measured using the hot disk method on as-cast samples having thickness of 8-10 mm or more, while these researchers measured the thermal conductivity of the composites by the laser flash method on 1 mm thick samples. Moreover, they have not described the exfoliated graphite settling in the epoxy resin at low loadings. Therefore, differences in local GNP concentrations might account for differences in conductivities. Furthermore, laser flash thermal conductivity data is dependent on correct measurements of specific heats and densities of the samples.

Another important difference between the present work and that of Ganguli et al. [23] and Debalak et al. [24] is the nature of the GNPs. They used exfoliated graphite as a starting material and they assumed that GNPs are formed during the process of mixing. Conversely, in present work GNPs are used to produce composites.

Nevertheless, a 20 wt. % GNP-15/RE composite produced by RM gave ~19-fold increase in thermal conductivity similar to that reported by Ganguli et al. [23] for 20 wt. % exfoliated graphite/epoxy composite. Yu et al. [11] reported a very high thermal conductivity of 1.45 W/m.K for a GNP/epoxy composite produced at ~10 wt. % loading but with platelets having width of 350 nm and thickness of 1.7 nm. In the present work, approximately similar thermal conductivity could be obtained for composites produced by RM at ~10 wt. % loading but with GNP-15s which have significantly large platelet width than GNPs used by Yu et al. [11].

The thermal conductivities of GNP/RE composites produced by RM are significantly higher than most of the commercial epoxy based TIMs (www.EPOTEK.com, dated 2017) but are achieved at 40-60 wt. % lower loadings of filler [11] and this makes them promising candidates for TIMs.

3.9 Electrical conductivity

The electrical conductivity of GNP/RE composites as a function of wt. % of GNP produced by RM, MM and SM measured in directions parallel (σ_{\parallel}) and perpendicular (σ_{\perp}) to that gravity acted during curing in the mould is presented in Fig. 8 and the data are also reported in Table 3.

The electrical resistivity of pure RE in the cured state is very high and its exact value was not determined due to a limitation of the instrument, which has detectable range up to 100 M Ω .

Fig. 8

Similar to thermal conductivities, RM also produced GNP/RE composites with the highest electrical conductivities than the other techniques. The composite produced by RM at 8 wt. % GNP-15 was insulating (as electrical resistance was not detectable by the meter which implies that the electrical conductivity was below percolation threshold of 10^{-6} S.m⁻¹) while all the composites produced at higher loadings were electrically conducting.

The electrical conductivities of composites produced by RM at 15 and 20 wt. % GNP-15 are slightly higher in the direction perpendicular than parallel to that in which gravity acted during curing (Fig. 8). This confirms higher orientation of GNPs in these composites as observed by XRD texture measurements (Fig. 4 (b & c)). The composite produced at 25 wt. % GNP-15 loading (by RM) has $\sim 4\times$ higher σ_{\parallel} than the composite produced at 20 wt. % loading (Fig. 8). The former also has $\sim 3.5\times$ higher σ_{\perp} than σ_{\parallel} . This result confirms that the 25 wt. % GNP-15/RE composite had higher texture than 20 wt. % GNP-15/RE composites (Fig. 4(d)). These results are contrary to thermal conductivities of roll milled composite where it was observed that thermal conductivity did not increase with loadings above 20 wt. % of GNP-15. It is clear from the electrical conductivity data that the thermal conductivity of 25 wt. % GNP-15/RE is much influenced by GNP-15 orientation,

but not the electrical conductivity which mainly depends on electron tunneling above the percolation threshold [10].

The GNP-15/RE composites at 20 wt. % produced by MM and SM reported previously [17] are effectively electrically insulating as can be seen from the very low electrical conductivities of these composites (Table 3 and Fig. 8). This comparison suggests that RM can produce composites with greater dispersion of GNPs than MM and SM techniques.

The effect of platelet width on the electrical conductivities of composites is also presented in Fig. 8 and Table 3. The GNP-5/RE composites produced by MM were completely insulating even at loadings up to 30 wt. % of GNP-5 [17]. Contrary to this, the composite produced by RM at 25 wt. % of GNP-5 was slightly electrically conducting. This again suggests that RM produces composites with greater dispersion than MM and SM.

Ganguli et al. [23] reported electrical conductivity of 4 S.m^{-1} for a 20 wt. % exfoliated graphite/epoxy composite produced by speed mixer. The electrical conductivity of a 20 wt. % GNP-15/RE composite produced here by RM is $8\times$ lower than Ganguli et al.'s corresponding composite. The large differences might be attributed to the type of epoxy matrix (based on curing agent).

The electrical conductivity measurements highlight the significance of processing technique in making electrically and thermal conducting composites. It is clear that the RM can produce highly electrically and thermally conducting composites. On the other hand, both MM and SM increases the thermal conductivity of composites up to 20 wt. % loading but leaves them electrically insulating (Table 3). Therefore, the study of processing techniques indicates that the best technique for producing GNP/RE composites is the RM, it also shows that different processing techniques/conditions can be used to vary or control transport properties of composites.

3.10 Compression testing of GNP/RE composites

The compression properties of GNP/RE composites as a function of wt. % GNPs produced by RM are presented in Fig. 9 and Table 4. For comparison compression properties of similar composites produced previously by MM and SM are also presented.

Fig. 9

The compressive modulus of pure RE at 20 % strain is 7.8 MPa indicating its good compliance. In the case of composites produced by RM, the addition of GNP-15s increases the compressive modulus and strength up to a loading of 20 wt. % but further additions at 25 wt. % loading reduces the compressive modulus and strength slightly. On the other hand, compressive strain to failure increases up to 15 wt. % GNP-15 loadings and then decreases with further additions. The compressive modulus and strength of 20 wt. % GNP-15/RE composites produced by RM increased by $\sim 2.6\times$ over that of pure RE. The compressive strength of 20 wt. % GNP-15/RE composite produced by RM is $\sim 25\%$ and 52% higher than the corresponding composites produced by MM and SM [17], respectively. This again suggests that the RM produced composites with better dispersion and distribution than other techniques. Overall, the decrease in compressive strain at loadings > 15 wt. % GNP-15s can be attributed to the much higher orientation of GNPs in the composites at these loadings which allows easy sliding of the overlapped sheets causing early crack initiation in the composite.

On the other hand, for otherwise equivalent composites, there is an increase in compressive strength for GNP-5/RE composite compared with GNP-15/RE composite at 25 wt. % loading. This behaviour can be explained by the fact that a smaller particle size can produce a stronger reinforcement effect than that from larger particles because there are more particles present in the former case. The GNP-5 particles can thus form more interfaces with each other and with the resin. These interfaces can interact with one another during the process of deformation and hence lead to an increase in the strength and reduction in compressive strain of the composite. The higher

compressive strength of 25 wt. % GNP-5/RE composites may also be due to the less GNP texture in these composites compared to equivalent GNP-15/RE composites (Fig. 4 (d & g)).

Although addition of GNPs increases the modulus of RE, despite this GNP/RE composites at their maximum workable loading are compliant materials. For instance, the modulus of 20 wt. % GNP-15/RE composite produced by RM is comparable to the commercial BN/silicone TIM having 65 wt. % BN (Table 4).

3.11 Hardness testing

The Shore hardnesses of GNP/RE composites as a function of wt. % of GNPs are also presented in Fig. 9 and Table 4. The Shore hardness of GNP/RE composite produced previously by MM and SM significantly increases with addition of GNPs at 20 and 25 wt. % loadings [17] attributed to the presence of agglomerated GNPs. However, in the case of composite produced by RM Shore hardness almost remained the same or decreased slightly with GNP-15 loadings up to 25 wt.%. The possible reasons for no increase in the hardness of GNP/RE composites could be a good dispersion of GNPs and well coated GNPs with the resin during roll milling.

3.12 Thermal contact resistance of GNP/RE composites as thermal interface adhesive

To qualify any material for TIMs applications, measurement of thermal contact resistance is very important. In this section a thermal contact resistance study of GNP/RE composites (produced by RM) as adhesives is presented.

3.12.1 Effect of GNPs loadings

The thermal contact resistances of pure RE and GNP/RE composite coatings measured as an adhesive layer between copper cylinders having smooth surfaces ($R_a = 0.03 \mu\text{m}$) at compressive stress of 0.032 MPa and temperature of $\sim 25^\circ\text{C}$ are presented in Table 5.

It can be observed from Table 5 that the thermal contact resistance of pure RE is $9.4 \times 10^{-5} \text{ m}^2 \cdot \text{K/W}$ at 15 μm bond line thickness. On the other hand, GNP-15/RE composites have $\sim 1.74 \times$ lower thermal contact resistance than pure RE at $\sim 4 \times$ thicker bond line. This suggests that the addition of GNPs improves the interfacial thermal transport performance of RE. The thermal contact resistance of 20 wt. % GNP-15/RE composite coating is $\sim 1.14 \times$ higher than the 15 wt. % GNP-15/RE coating at approximately equivalent bond line thickness. This might be due to the slightly lower viscosity (Fig. 1) of the latter coating which resulted in a better interfacial contact with the substrate. On the other hand, the thermal contact resistance of 25 wt. % GNP-5/RE composite is $\sim 1.44 \times$ and $1.26 \times$ higher than 15 and 20 wt. % GNP-15/RE composite coating, respectively, at approximately equivalent bond line thickness. It was observed that the 25 wt. % GNP-5/RE composite dispersion had significantly lower viscosity than 15 wt. % GNP-15/RE composite and this should result in a better interfacial contact with the substrate and thus more conformable coating. However, the inferior performance of 25 wt. % GNP-5/RE coating compared to 15 wt. % GNP-15/RE coating might be due to its lower thermal conductivity (Table 3).

3.12.2 Effect of particle size of GNPs and surface roughness of substrate

To study the particle size effect on thermal contact resistance, the total thermal contact resistances of 25 wt. % GNP-5/RE and 15 wt. % GNP-15/RE composites versus coating thicknesses applied between the smooth surfaces (cured in-situ under pressure) measured at 0.032 MPa compressive stress and $\sim 25 \text{ }^\circ\text{C}$ are presented in Fig. 10. The thermal contact resistances of these coatings measured between rough surfaces are also presented in Fig. 10. The summary of results obtained from linear fitting of the data is presented in Table 6.

Fig. 10

It can be seen from Fig. 10 that a minimum thickness of $\sim 20 \mu\text{m}$ was achieved for both 25 wt. % GNP-5/RE and 15 wt. % GNP-15/RE. This was obtained by applying the pressure of $\sim 0.1 \text{ MPa}$ on the copper cylinders before curing. The lowest thermal contact resistance of $\sim 2.4 \times 10^{-5} \text{ m}^2 \cdot \text{K/W}$ is

obtained for both 25 wt. % GNP-5/RE and 15 wt. % GNP-15/RE coatings at equivalent bond line thickness of 20 μm . However, at thick bond lines, e.g., 85 μm , the thermal contact resistance of the 25 wt. % GNP-5/RE coating is $\sim 1.21\times$ higher than the 15 wt. % GNP-15/RE coating. The better interfacial thermal transport performance of the latter coating is attributed to its $\sim 33\%$ higher thermal conductivity (according to steady state method, Table 6). This result also suggests that at thick bond lines thermal conductivity is more influential than at thin bond lines.

The total thermal contact resistance of both the 25 wt. % GNP-5/RE and the 15 wt. % GNP-15/RE composite coatings is almost the same on rough and smooth surfaces at approximately equivalent coating thicknesses. However, it can be observed from Table 6 that total geometric thermal interfacial resistance of coating with smaller particle size is significantly lower than a coating with large particle size. This result suggests that the 25 wt. % GNP-5/RE composite coating is more conformable than 15 wt. % GNP-15/RE coating and forms better contact with the mating surfaces might be due to its lower viscosity.

The thermal conductivities of 25 wt. % GNP-5/RE and 15 wt. % GNP-15/RE composites measured by hot disk method on bulk composites were 46 and 63 %, respectively, higher than their coatings measured according to steady state method. This might be the effect of higher orientation of GNPs parallel to the interfacial plane due to their curing under pressure.

It is also shown in Fig. 10 that thermal contact resistance of uncured 25 wt. % GNP-5/RE composite is approximately same as for the cured coating measured under similar conditions. This shows that cured coatings can perform similar to the uncured coatings. This is because in the uncured state they can flow and fill up the cavities of the surface same like the pastes and after curing they stick to the surface more strongly.

3.12.3 Effect of pressure and temperature

The total thermal contact resistance of a 25 wt. % GNP-5/RE coating as a function of applied pressure for the bond line thickness of $123 \pm 5 \mu\text{m}$ measured between smooth surfaces at $\sim 25 \text{ }^\circ\text{C}$ is

presented in Fig. 11. The effect of temperature on the thermal contact resistance is also presented in Fig. 11. The thermal contact resistance of 25 wt. % GNP-5/RE coating has not changed with application of pressure in the range of 0.032-0.16 MPa. This is a typical behaviour for an adhesive as after curing it bonds the mating surface. However, the thermal contact resistance increased by ~8 % with increase of temperature from 25 to 40 °C as the thermal conductivity increases with increase of temperature due to increased scattering of phonons.

Fig. 11

3.12.4 Comparison of GNP/RE composite TIMs with other TIMs

The comparison of GNP/RE composite with the commercial TIMs and literature data on TIMs is presented in Table 7. The thermal contact resistance of commercial paste (Matrix II) was measured on the rig under the similar conditions as that of GNP/RE composites [21]. This paste has very low thermal contact resistance ($4.6 \times 10^{-6} \text{ m}^2 \cdot \text{K/W}$) under a pressure of 0.032 MPa (it was not easy to measure bond line thickness of the paste, a crude measurement suggests that it may be 10-20 μm). The thermal contact resistance of 15 wt. % GNP-15/RE composite as adhesive is ~4.8 \times higher than the Matrix II paste at approximately equivalent bond line thickness. This shows that the GNP/RE adhesive cannot outperform Matrix II paste. On the other hand, it can also be observed from Table 7 that thermal contact resistances of GNP and CB-pastes reported by Lin et al. [6] are 3 \times and 7.4 \times , respectively, higher than 15 wt. % GNP-15/RE composite at a thick bond line of ~50 μm . These results clearly show that GNP/RE adhesives perform much better at thick bond lines.

Comparison of the interfacial thermal transport performance of 15 wt. % GNP-15/RE composites with equivalent 15 wt. % GNP-15/silicone composites (Table 7) reported previously in [21] shows that the thermal contact resistance of the latter is 2 \times higher than the former at a bond line thickness of ~18 μm . This result suggests that RE based coatings form better contacts with the substrate perhaps due to the stronger adhesive nature of RE than

silicone and this contributes to the improved performance of 15 wt. % GNP-15/RE composite over corresponding GNP/silicone composite.

The thermal contact resistance of commercial BN/silicone TIM (EPM 2490) is 1.17× higher than 15 wt. % GNP-15/RE composite at a bond line thickness of 95 μm. This shows that the interfacial thermal transport performance of GNP/RE composites as TIM adhesives is not only better than commercial adhesive but is also obtained at 50-60 % less loading of the filler.

The comparison of GNP/RE composite adhesives with commercial TIM adhesive and CB- and GNP-thermal pastes reported in [6, 8] shows that these composites can certainly perform much better at thick bond lines due to their high thermal conductivity. However, they are unable to outperform commercial thermal paste at thin bond lines.

3.12.5 Thermal contact resistance of thermal pads

Thermal pads of selected GNP/RE composites were produced by compression moulding (shown in the inset of Fig.12). These pads had a very high GNP texture as discussed in texture Section 3.5 (Fig. 6(d & f)). The average thicknesses of these pads were in the range of 0.6-0.7 mm. The thermal contact performance of these pads was measured according to the steady state method on the thermal contact resistance measurement rig by sandwiching them between smooth surfaces of copper cylinders ($R_a = 0.06 \mu\text{m}$). The thermal contact resistances of these pads were measured as a function of applied pressure (0.032-0.16 MPa) and are presented in Fig. 12. The thermal contact resistance of a commercial thermal pad, a product of Dow Corning Company, was also measured on the rig. A thermal pad of commercial TIM, EPM 2490, was also fabricated in the lab by the same method that was used to fabricate GNP/RE pads and tested on the rig.

Fig. 12

It can be observed from Fig. 12 that the application of pressure in the range of 0.032-0.16 MPa slightly decreases the thermal contact resistance of these pads. The applied pressure improves the interfacial contact of the pad with the substrate and this results in an overall decrease in thermal

contact resistance. The best interfacial thermal transport performance is given by the Dow Corning's silicone based pad and this might be attributed to its sticky nature which forms much better contact with the substrate. The thermal contact resistance of a commercial 65 wt. % BN/silicone (EPM 2490) pad is $4.3 \times 10^{-4} \text{ m}^2 \cdot \text{K/W}$ at a pressure of 0.032 MPa and this decreases slightly with increase of pressure. The 20 wt. % GNP-15/RE composite pad produced by RM has significantly lower thermal contact resistance than all other GNP/RE pads. However, the thermal contact resistance of this pad is $\sim 1.11 \times$ higher than the EPM pad at 0.032 MPa but with increase of pressure its thermal contact resistance became almost the same as that of the EPM pad. This shows that conformability of GNP/RE pad improves with an increase of applied pressure. The thermal contact resistance of 20 wt. % GNP-15/RE composite pad produced by MM is $1.14 \times$ higher than the equivalent pad produced by RM. The better interfacial thermal transport performance of a pad produced by RM again suggests superior dispersion quality of the RM compared to the MM. The thermal contact resistance of 25 wt. % GNP-5/RE composite (produced with smaller particles GNP-5) is also $\sim 1.15 \times$ higher than GNP-15/RE pads produced by RM.

The performance of GNP-pads is also affected by the high texture of GNPs because the heat conduction direction is preferentially through-plane of the GNPs present in the composite pads. Perhaps, the performance of GNP-pads could be improved by making the pads from the composite which was cured without the application of pressure (to avoid high texture) and also by applying a sticky coating on their surface like commercial Dow Corning pads. The thermal contact resistance of 20 wt. % GNP-15/RE pad produced by RM is although 35 % higher than the commercial Dow Corning pad but it is still comparable to the BN/silicone pad. This suggests that GNP-pads could be potential candidates for thermal pad TIMs applications as they not only give comparable performance to commercial TIMs but can also save cost by offering this performance at relatively less loading of the filler.

4. Conclusions

Composites produced by RM have significantly increased transport and mechanical properties compared to the those produced with MM and SM which is attributed to the greater dispersion of GNPs obtained due to the high shearing and crushing action of the RM. Composites produced by RM have uniform dispersion of GNPs at low and high loadings. In contrast, both MM and SM were unable to produce composites with good dispersion at low loadings which resulted in high concentration gradient in ~10 mm as-cast samples. RM produces the composites with lower texture at low loadings but this propensity of RM decreases with increasing GNP loadings.

The thermal conductivity of GNP/RE composites increases with an increase of wt. % of GNPs and with the increase of particle size, as both of these factors favour establishment of improved thermal pathways. The thermal conductivity of GNP-15/RE composite (3.29 W/mK) produced by RM increased by 19-fold compared to the pure RE (0.17 W/m.K) at 20 wt. % GNP-15s. The thermal conductivity of GNP-5/RE composite (2.36 W/m.K) increased by ~14-fold compared to pure RE at 35 wt. % of GNP-5s. Compression testing showed that the GNP/RE composites retained good compliance, as their modulus at 20 wt. % loadings is comparable to commercial BN/silicone TIM.

The thermal contact resistance of GNP/RE was significantly higher than the commercial paste but their interfacial thermal transport performance was better at thick bond lines than that of GNP-pastes reported in the literature. The interfacial thermal transport performance of GNP/RE composite was also better than GNP/silicone composite which is attributed to the strong adhesive nature of RE. The GNP/RE composites produced with small and large particles performed almost similar at thin bond lines but at thick bond lines composite produced with large particle size had much better interfacial thermal transport performance due to its higher thermal conductivity.

The GNP-15/RE composite thermal pad produced by roll mil at 20 wt. % loading has significantly lower thermal contact resistance than other GNP/RE pads. Its thermal contact resistance decreased

with increase of applied pressure and is comparable to commercial BN/silicone, EPM 2490 pad, but it was unable to outperform commercial Dow Corning thermal pad.

GNP/RE composites with their high thermal conductivity, low electrical conductivity, high compliance and lower thermal contact resistance at thick bond lines as thermal interface adhesive or thermal pads meet the basic requirements of thermal interface materials and are promising candidates for thermal interface applications.

Acknowledgements

The authors would like to thank EPSRC, UK, Morgan Advanced Materials, UK and Higher Education Commission of Pakistan (grant No. 20-3283) for providing financial support for carrying out this research work.

References

1. D. D. L. Chung, *Journal of Materials Engineering and Performance* **10**, 56-59 (2001).
2. J. P. Gwinn and R. L. Webb, *Microelectronics Journal* **34**, 215-222 (2003).
3. R. Linderman, T. Brunschwiler, B. Smith, et al., *THERMINIC 2007* (2007).
4. F. Sarvar, D. C. Whalley and P. P. Conway, *IEEE ,2006 Electronics Systemintegration Technology Conference Dresden,Germany*, 1292-1302 (2006).
5. K. C. Otiaba, N. N. Ekere, R. S. Bhatti, et al., *Microelectronics Reliability* **51**, 2031-2043 (2011).
6. C. Lin and D. D. L. Chung, *Carbon* **47**, 295-305 (2009).
7. J. Liu, T. Wang, B. Carlberg, et al., *Electronics System-Integration Technology Conference* **2**, 351-358 (2008).
8. C.-K. Leong, Y. Aoyagi and D. D. L. Chung, *Carbon* **44**, 435-440 (2006).
9. A. A. Balandin, S. Ghosh, W. Bao, et al., *Nano letters* **8** (3), 902-907 (2008).
10. M. H. Al-Saleh and U. Sundararaj, *Carbon* **47** (1), 2-22 (2009).
11. A. Yu, P. Ramesh, M. E. Itkis, et al., *J. Phys. Chem. C* **111**, 7565-7569 (2007).
12. D. Fabris, M. Rosshirt, C. Cardenas, et al., *Journal of Electronic Packaging* **133** (2), 020902 (2011).
13. Z. Lingbo, D. W. Hess and P. Wong, in *Electronic Components and Technology Conference, 2007. ECTC '07. Proceedings. 57th, 2007*, p. 2006-2010.
14. K. M. F. Shahil and A. A. Balandin, *Solid State Communications* **152** (15), 1331-1340 (2012).
15. B. Li and W.-H. Zhong, *Journal of Materials Science* **46**, 5595-5614 (2011).
16. Q. Mu and S. Feng, *Thermochimica Acta* **462**, 70-75 (2007).
17. M. A. Raza, A. V. K. Westwood and C. Stirling, *Materials Chemistry and Physics* **132** (1), 63-73 (2012).
18. M. A. Raza, A. Westwood and C. Stirling, *Carbon* **50** (1), 84-97 (2012).
19. M. A. Raza, A. V. K. Westwood, A. P. Brown, et al., *Composites Science and Technology* **72** (3), 467-475 (2012).
20. M. A. Raza, A. Westwood, A. Brown, et al., *Carbon* **49** (13), 4269-4279 (2011).

21. M. Raza, A. Westwood, A. Brown, et al., *Journal of Materials Science: Materials in Electronics*, 1-9 (2012).
22. M. A. Raza, A. Westwood and C. Stirling, *Materials & Design* **85**, 67-75 (2015).
23. S. Ganguli, A. K. Roy and D. P. Anderson, *Carbon* **46**, 806-817 (2008).
24. B. Debelak and K. Lafdi, *Carbon* **45**, 1727–1734 (2007).

Table. 1 Summary of the dispersion quality and morphology of GNP/epoxy composites produced by various techniques observed by SEM.

Composite	Fabrication method	Dispersion quality	Comments
8 wt. % GNP-15/RE	MM [17]	Poor	MM unable to break agglomerates at low loading. High concentration gradient (from top to bottom) in as-cast sample due to particle settling in low viscosity resin.
20 wt. % GNP-15/RE	MM [17]	Good	GNPs are uniformly distributed, few agglomerates observed, particles form interconnects.
20 wt. % GNP-15/RE	SM [17]	Fair	Thicker GNPs agglomerates than those observed in equivalent composite produced by MM. GNPs form interconnects.
20 wt. % GNP-15/glassy epoxy	MM [17]	Good	Few agglomerates, plenty of voids observed.
8 wt. % GNP-15/RE	RM	Excellent	No concentration gradient, some interconnects observed.
15 wt. % GNP-15/RE	RM	Excellent	Many interconnects observed.
20 wt. % GNP-15/RE and 25 wt. % GNP-15/RE	RM	Excellent	Plenty of interconnects, very small segments of matrix between the GNPs observed.

Table 2. Average thicknesses of GNPs determined from XRD (0002) peak-broadening analysis.

Samples	(0002) d spacing (°A)	Average thickness GNPs (nm)	Range of data * (nm)
GNP-15 (as received)	3.37	59	2
GNP-5 (as received)	3.38	29	3
8 wt. % GNP-15/RE by RM	3.35	30	5
20 wt. % GNP-15/RE by RM	3.36	33	4
25 wt. % GNP-15/RE by RM	3.37	36	1
25 wt. % GNP-5/RE by RM	3.37	23	2
20 wt. % GNP-15/RE by SM	3.35	31	4
20 wt. % GNP-15/RE by MM	3.35	30	2
25 wt. % GNP-15/RE by MM	3.38	33	1
25 wt. % GNP-5/RE by MM	3.38	22	2

* Data range is obtained by testing at least 2-3 specimens of each sample

Table 3. Thermal and electrical conductivities of pure epoxy and GNP/epoxy composites.

Material	Fabrication method	*Thermal Conductivity W/m.K	†Electrical conductivity ($\sigma_{ }$) S.m⁻¹
Pure RE (RE)	MM	0.176 ± 0.001	Insulating
8 wt. % GNP-5/RE	MM	0.494 ± 0.302	Insulating
15 wt. % GNP-5/RE	MM	0.573 ± 0.272	Insulating
20 wt. % GNP-5/RE	MM	0.772 ± 0.157	Insulating
25 wt. % GNP-5/RE	MM	1.12 ± 0.008	Insulating
30 wt. % GNP-5/RE	MM	1.63 ± 0.02	Insulating
15 wt. % GNP-5/RE	SM	0.593 ± 0.309	Insulating
20 wt. % GNP-5/RE	SM	0.765 ± 0.234	Insulating
25 wt. % GNP-5/RE	RM	1.47 ± 0.001	$(4.42 \pm 3) \times 10^{-6}$
35 wt. % GNP-5/RE	RM	2.36 ± 0.003	0.55 ± 0.2
8 wt. % GNP-15/RE	MM	0.634 ± 0.443	Insulating
15 wt. % GNP-15/RE	MM	0.862 ± 0.488	Insulating
20 wt. % GNP-15/RE	MM	1.65 ± 0.06	$(8.75 \pm 9) \times 10^{-5}$
25 wt. % GNP-15/RE	MM	2.35 ± 0.001	0.42 ± 0.03
20 wt. % GNP-15/RE	SM	1.53 ± 0.05	$(1.561 \pm 2) \times 10^{-4}$
25 wt. % GNP-15/RE	SM	2.15 ± 0.007	$(4.51 \pm 3) \times 10^{-4}$
8 wt. % GNP-15/RE	RM	1.13 ± 0.024	Insulating
15 wt. % GNP-15/RE	RM	1.75 ± 0.004	0.01 ± 0.01
20 wt. % GNP-15/RE	RM	3.29 ± 0.038	0.5 ± 0.2
25 wt. % GNP-15/RE	RM	3.17 ± 0.11	1.9 ± 0.4

*Each value is an average of 2-3 measurements and is followed by data range. † Error is obtained by measurements on 4-5 specimens of each sample.

Table 4. Compression and hardness properties of pure RE and GNP/RE composites.

Material	Fabrication method	Compressive modulus (at 20 % strain) MPa	Compressive strength at failure MPa	Compressive strain at failure (%)	Shore hardness (Scale A)
Pure RE	MM	7.8 ± 0.52	2.48 ± 0.68	27.5 ± 4.94	59 ± 2
8 wt. % GNP-15/RE	RM	12.84 ± 0.56	5.18 ± 0.2	37.2 ± 0.14	58 ± 2
15 wt. % GNP-15/RE	RM	15.23 ± 0.09	6.29 ± 0.64	38.83 ± 1.13	57 ± 1
20 wt. % GNP-15/RE	RM	21.23 ± 1.23	6.61 ± 0.8	33.64 ± 5.23	56 ± 2
25 wt. % GNP-15/RE	RM	20.16 ± 1.81	5.3 ± 0.88	29.06 ± 1.61	55 ± 2
25 wt. % GNP-5/RE	RM	23.42 ± 1.57	8.93 ± 0.89	34.01 ± 1.53	56.6 ± 2
35 wt. % GNP-5/RE	RM	32.3 ± 5.54	9.01 ± 3.1	27.45 ± 3.2	59 ± 3
20 wt. % GNP-15/RE	MM	17.73 ± 0.37	5.27 ± 0.08	33.73 ± 0.77	78 ± 3
25 wt. % GNP-15/RE	MM	20.53 ± 1.56	5.14 ± 0.72	27.5 ± 3.67	81 ± 4
25wt. % GNP-5/RE	MM	21.18 ± 1.08	6.08 ± 0.02	30.22 ± 1.3	76 ± 2
30 wt. % GNP-5/RE	MM	27.37 ± 1.09	7.56 ± 0.03	29.76 ± 0.82	81 ± 3
20 wt. % GNP-15/RE	SM	18.68 ± 2.76	4.33 ± 0.2	28.17 ± 1.1	76 ± 3
25 wt. % GNP-15/RE	SM	20.4 ± 2.43	5.46 ± 0.94	30.16 ± 3.66	83 ± 1
EPM 2490 (Commercial TIM, a product of Nusil Ltd.)	-	18.72 ± 3.92	7.5 ± 1.4	51.61 ± 2.86	81.2 ± 2.1

Errors for all compressive properties were obtained by testing 3-4 samples of each material. Shore hardnesses were averaged from at least 5 measurements on each composite sample.

Table 5. The thermal contact resistances of pure RE and GNP/RE composites measured at ~25 °C and 0.032 MPa compressive stress.

Composite coating	Bond line thickness $\pm 5 \mu\text{m}$	Total thermal contact resistance $\text{m}^2.\text{K}/\text{W}$
Pure RE	15	9.4×10^{-5}
15 wt. % GNP-15/RE	55	4.7×10^{-5}
20 wt. % GNP-15/RE	54	5.4×10^{-5}
25 wt. % GNP-5/RE	60	6.8×10^{-5}

Table 6. Thermal conductivity and geometric thermal interfacial resistance of GNP/RE composite coatings produced by RM measured between smooth surfaces under 0.032MPa compressive stress at ~ 25 °C.

Material	Equation of linear fit of total thermal resistance vs. thickness data	Total Geometric thermal interfacial resistance $\text{m}^2.\text{K}/\text{W}$	Thermal conductivity (steady state method) $\text{W}/\text{m.K}$	Thermal conductivity (Hot disk method) of composite $\text{W}/\text{m.K}$
15 wt. % GNP-15/RE	$y = 0.83 x + 8.44 \times 10^{-6}$, $R^2 = 0.93$	8.44×10^{-6}	1.2	1.75
25 wt. % GNP-5/RE	$y = 1.11 x + 1.36 \times 10^{-6}$, $R^2 = 0.99$	1.36×10^{-6}	0.9	1.47

Table 7. Comparison of thermal contact resistance of GNP/RE composites with other TIMs.

TIM	Reference	Pressure (MPa)	Bond line thickness (μm)	Thermal contact resistance ($\text{m}^2\cdot\text{K}/\text{W}$)
Matrix II paste (commercial TIM) www.tim-consultants.com	Measured in the lab under same conditions at which GNP/RE studied (see Appendix 7.3)	0.032	10-20	4.6×10^{-6}
15 wt. % GNP-15/RE adhesive produced by RM	Present study (predicted on the basis of linear fit equation)	0.032	18	2.2×10^{-5}
1.2 vol.% GNP-paste	[6]	0.46	50	1.67×10^{-4}
15 vol.% carbon black(Tokai) paste	[6]	0.46	50	4×10^{-4}
15 wt. GNP-15/RE adhesive produced by RM	Present study (predicted on the basis of linear fit equation and increased by 10 % to be at a consistent temperature with [6])	0.032	50	5.4×10^{-5}
15 wt. % GNP-15/RE adhesive produced by RM	Present study (estimated on the basis of linear fit equation)	0.032	95	8.6×10^{-5}
65 wt. %BN/silicone (EPM 2490) adhesive (EX. Nusil)	Measured in our lab under the same conditions at which GNP/RE studied	0.032	95	1.01×10^{-4}
15 wt. % GNP-15/silicone	[21]	0.032	18	4.3×10^{-5}

Fig. Captions

Fig. 1. Viscosity profiles of pure RE and GNP-epoxy dispersions before curing produced by MM and RM (it was not possible to continue the flow test of the 20 wt. % GNP-15/RE dispersion produced by RM at shear rates $>15 \text{ s}^{-1}$ due to equipment limitations which depend on the viscosity of the sample).

Fig. 2. SEM images of GNP-15/RE composite produced by RM at loading of (a & b) 8 wt. % (c & d) 15 wt. % (e & f) 20 wt. % (g & h) 25 wt. % and (i & j) 25 wt. % GNP-5/RE composite, arrows point towards GNPs in the matrix.

Fig. 3. XRD plots of the (0002) peaks of the as-received GNPs and GNP/RE composites produced by various processing techniques.

Fig. 4. Pole figures of composites produced by RM (a) 8 wt. % GNP-15/RE (b) 15 wt. % GNP-15/RE (c) 20 wt. % GNP-15/RE (d) 25 wt. % GNP-15/RE (e) 35 wt. % GNP-15/RE (f) 60 wt. % GNP-15/RE (g) 25 wt. % GNP-5/RE (h) 20 wt. % GNP-15/RE composite cured under compression.

Fig. 5. Effect of passing the 20 wt. % GNP-15/RE dispersion through roll mil on texture of the composites (a) 5 passes (b) 10 passes (c) 15 passes.

Fig. 6. Pole figures of 20 wt. % GNP-15/RE composites produced by (a) RM (b) SM (c) MM (d) 20 wt. % GNP-15/RE composite produced by MM is cured under pressure (e) 25 wt. % GNP-5/RE composite produced by MM (f) 25 wt. % GNP-5/RE composite produced by MM cured under pressure.

Fig. 7. Room temperature thermal conductivity of (a) GNP-15/RE and (b) GNP-5/RE composites produced by RM, MM and SM as a function of wt. % of GNPs with corresponding data for glassy epoxy composite for comparison. Each line is passing through the average values for given wt. % obtained by an average of 2-3 measurements. The additional points indicate the data ranges for given wt. % of GNPs, which in most of the cases were obtained by measuring the thermal conductivities on the bottom (data points above average values) and top sections (data points below average values) of the as-cast samples.

Fig. 8. Electrical conductivities of GNP-15/RE as a function of wt. % GNP-15s produced by RM, MM, and SM. Effects of platelet size is also presented. Errors are determined by measurements on 4-5 different specimens of each material.

Fig. 9. Compressive properties and Shore hardnesses of GNP/RE composites as a function of wt. % of GNPs produced by RM, MM and SM. Data is averaged by testing 3-4 specimens of each material.

Fig. 10. Total thermal contact resistance vs. coating thickness of (a) 25 wt. % GNP-5/RE (RE) (b) 15 wt. % GNP-15/RE composite produced by RM measured on smooth and rough surfaces at 0.032 MPa compressive stress. The thermal contact resistance of 25 wt. % GNP-5/RE coating in an uncured state measured on smooth is also presented (a). The thermal contact resistance of 20 wt. % GNP-15/RE on smooth surface and 25 wt. % GNP-15/RE coating on rough surface is also presented (b). Linear fit and the equation of linear fit are also shown. Errors are obtained from at least 20 data points recorded under steady state conditions of 20-40 min.

Fig. 11. Total thermal contact resistance of 25 wt. % GNP-5/RE between smooth surface as a function of applied pressure and temperature. Errors are obtained from at least 20 data points recorded under steady state conditions of 20-40 min.

Fig. 12. Thermal contact resistance vs. applied pressure of GNP/RE and commercial pads measured at ~42 °C between smooth copper cylinders. Standard deviations are obtained from at least 20 data points obtained under steady state conditions of 20-40 min. Inset shows that 20 wt. % GNP-15/RE pad is easily foldable like commercial silicone (EPM 2490) thermal pad.

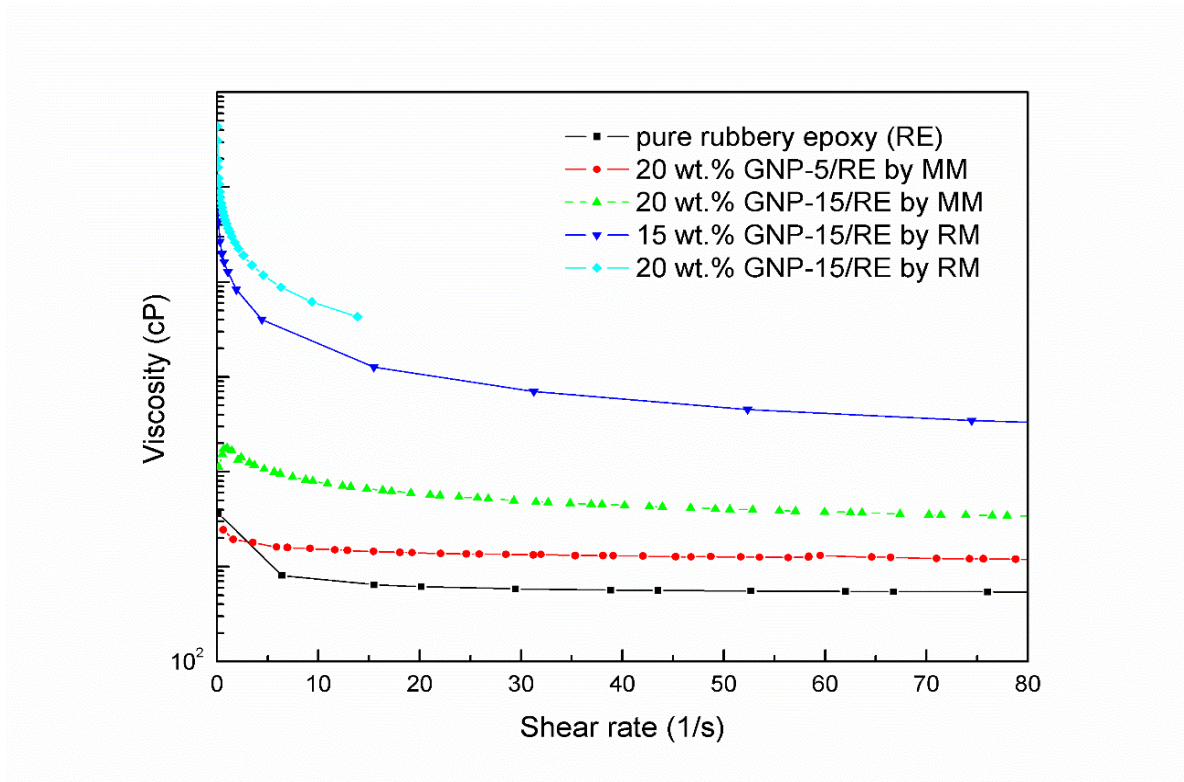


Fig. 1. Viscosity profiles of pure RE and GNP-epoxy dispersions before curing produced by MM and RM (it was not possible to continue the flow test of the 20 wt. % GNP-15/RE dispersion produced by RM at shear rates $>15 \text{ s}^{-1}$ due to equipment limitations which depend on the viscosity of the sample).

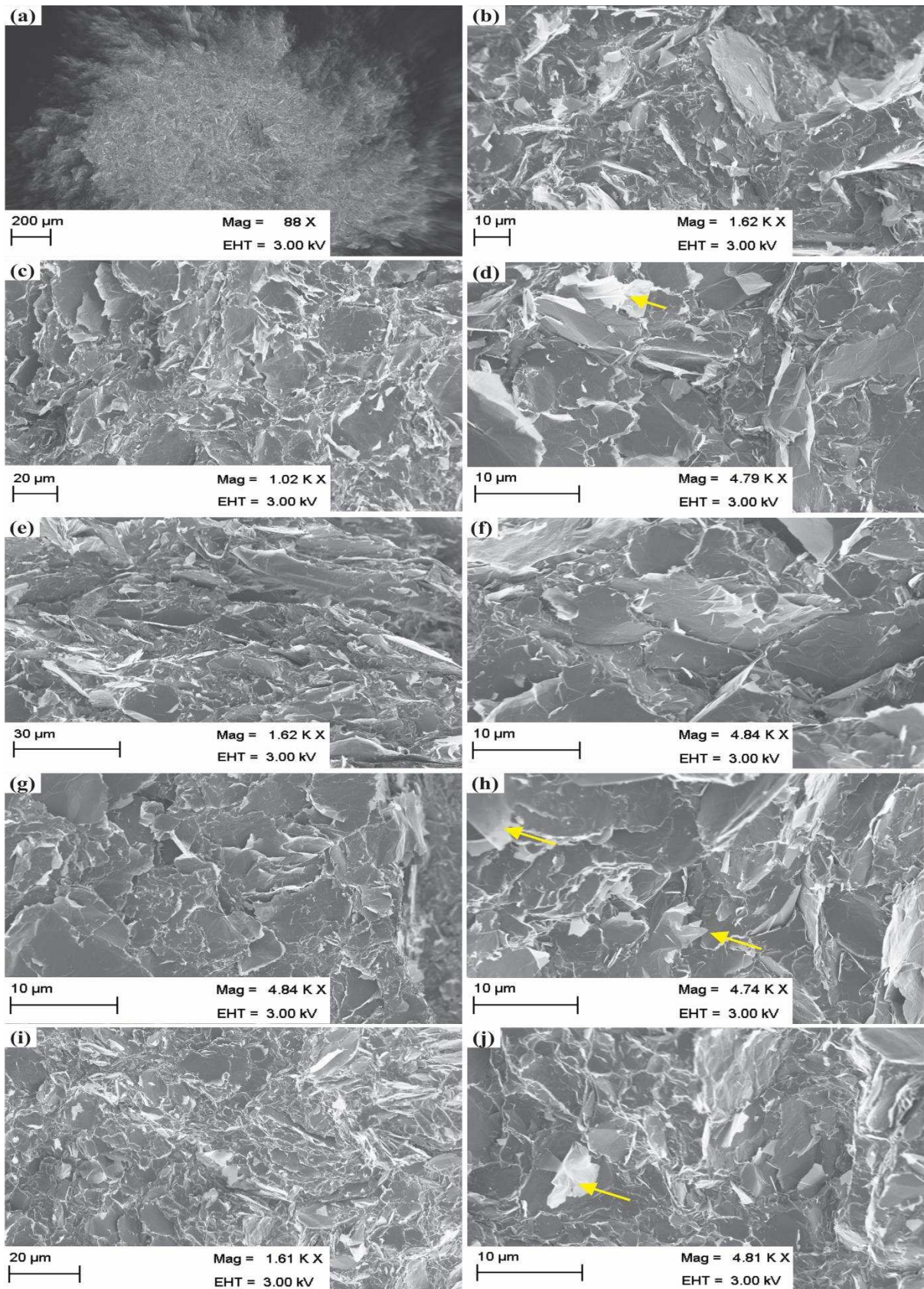


Fig. 2. SEM images of GNP-15/RE composite produced by RM at loading of (a & b) 8 wt. % (c & d) 15 wt. % (e & f) 20 wt. % (g & h) 25 wt. % and (i & j) 25 wt. % GNP-5/RE composite, arrows point towards GNPs in the matrix.

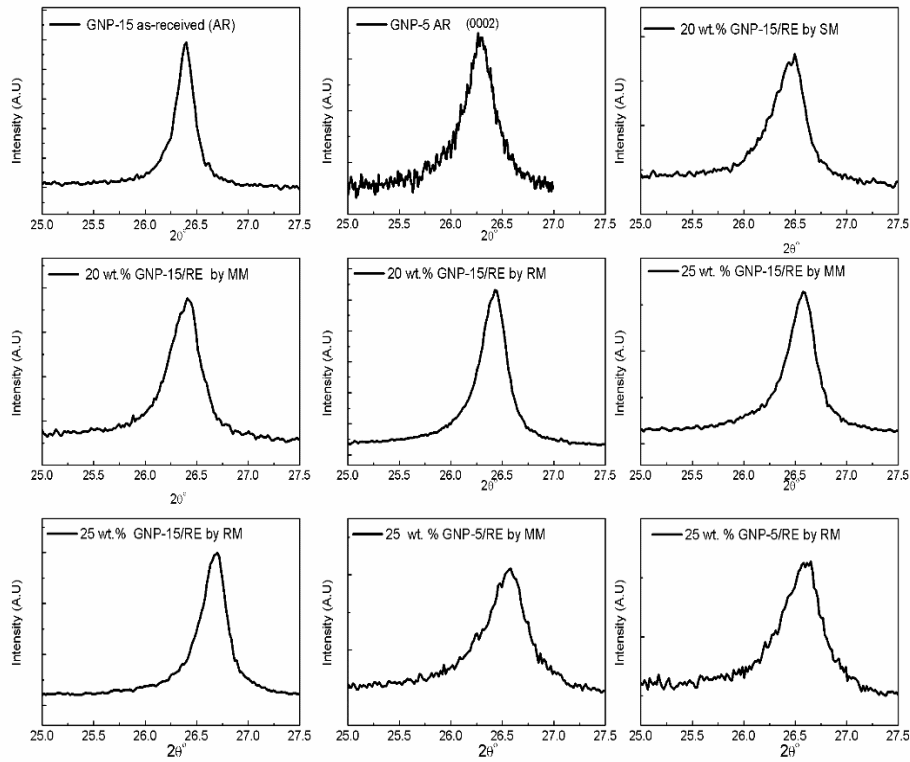


Fig. 3. XRD plots of the (0002) peaks of the as-received GNPs and GNP/RE composites produced by various processing techniques.

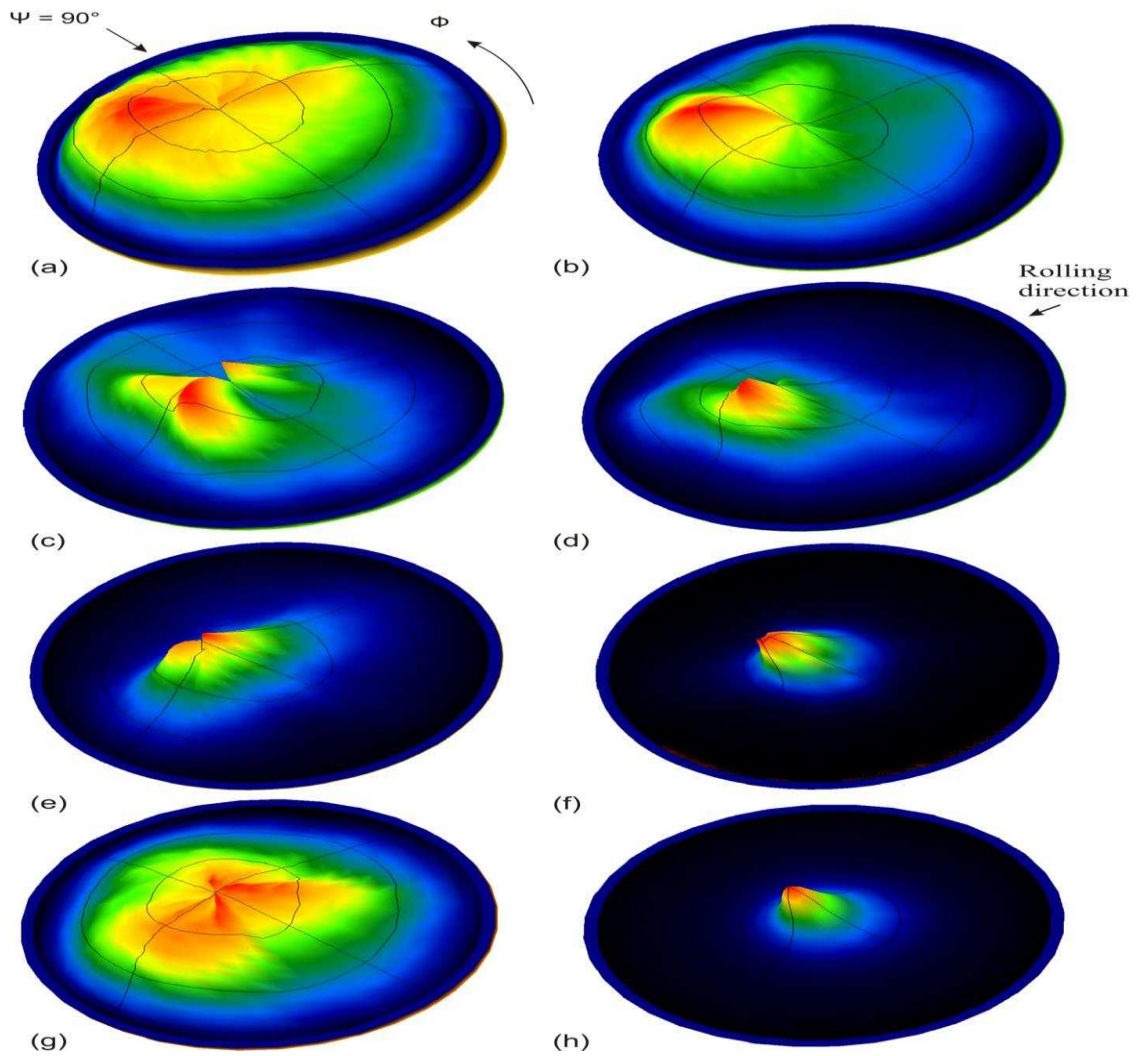


Fig. 4. Pole figures of composites produced by RM (a) 8 wt. % GNP-15/RE (b) 15 wt. % GNP-15/RE (c) 20 wt. % GNP-15/RE (d) 25 wt. % GNP-15/RE (e) 35 wt. % GNP-15/RE (f) 60 wt. % GNP-15/RE (g) 25 wt. % GNP-5/RE (h) 20 wt. % GNP-15/RE composite cured under compression.

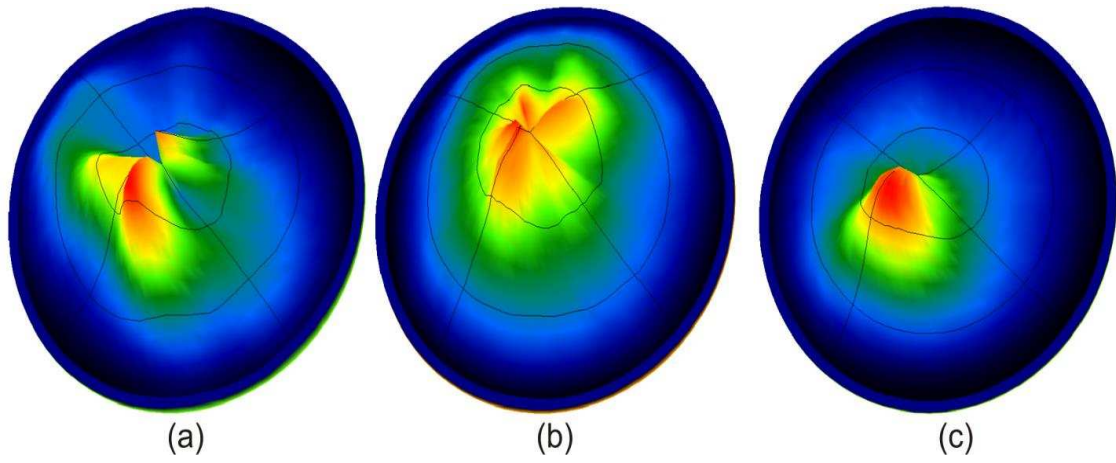


Fig. 5. Effect of passing the 20 wt. % GNP-15/RE dispersion through roll mil on texture of the composites (a) 5 passes (b) 10 passes (c) 15 passes.

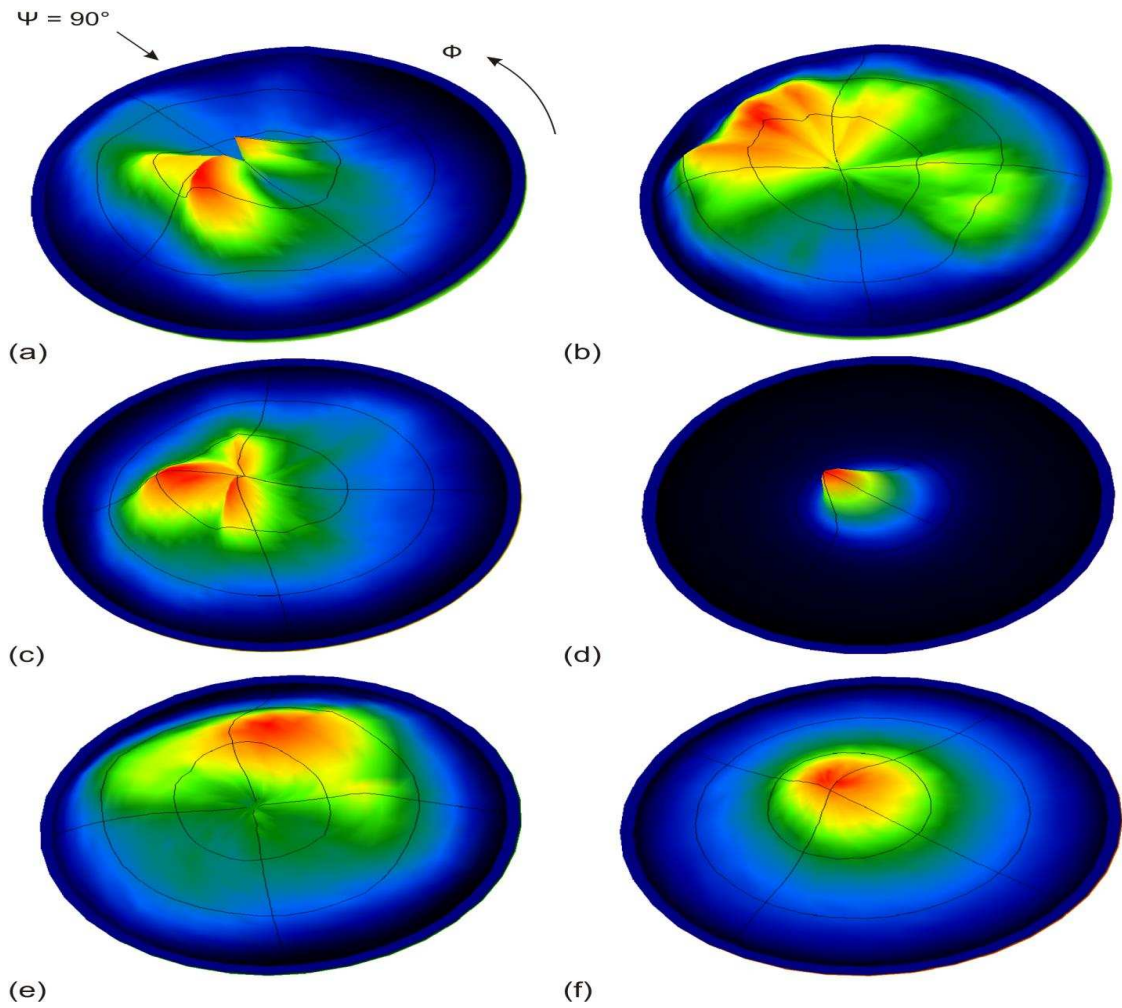


Fig. 6. Pole figures of 20 wt. % GNP-15/RE composites produced by (a) RM (b) SM (c) MM (d) 20 wt. % GNP-15/RE composite produced by MM is cured under pressure (e) 25 wt. % GNP-5/RE composite produced by MM (f) 25 wt. % GNP-5/RE composite produced by MM cured under pressure.

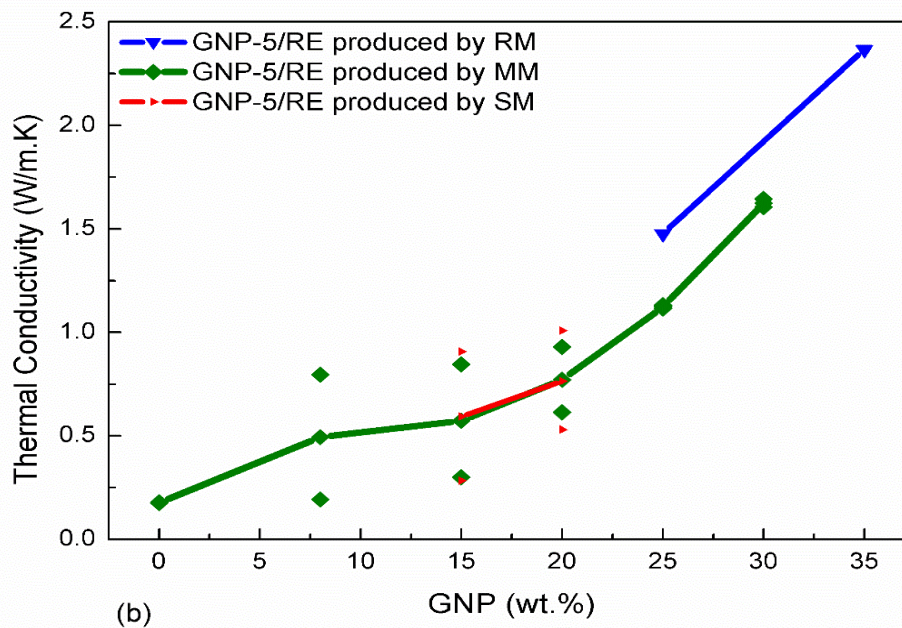
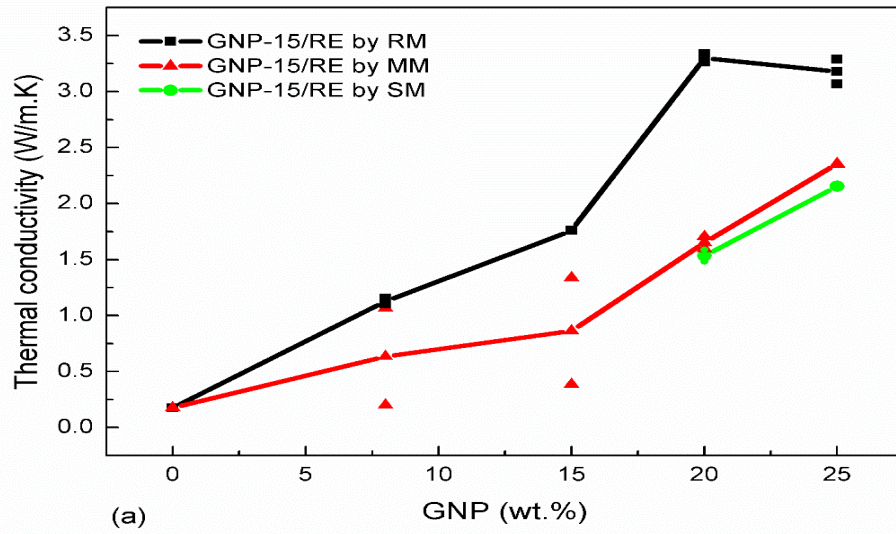


Fig. 7. Room temperature thermal conductivity of (a) GNP-15/RE and (b) GNP-5/RE composites produced by RM, MM and SM as a function of wt. % of GNPs with corresponding data for glassy epoxy composite for comparison. Each line is passing through the average values for given wt. % obtained by an average of 2-3 measurements. The additional points indicate the data ranges for given wt. % of GNPs, which in most of the cases were obtained by measuring the thermal conductivities on the bottom (data points above average values) and top sections (data points below average values) of the as-cast samples.

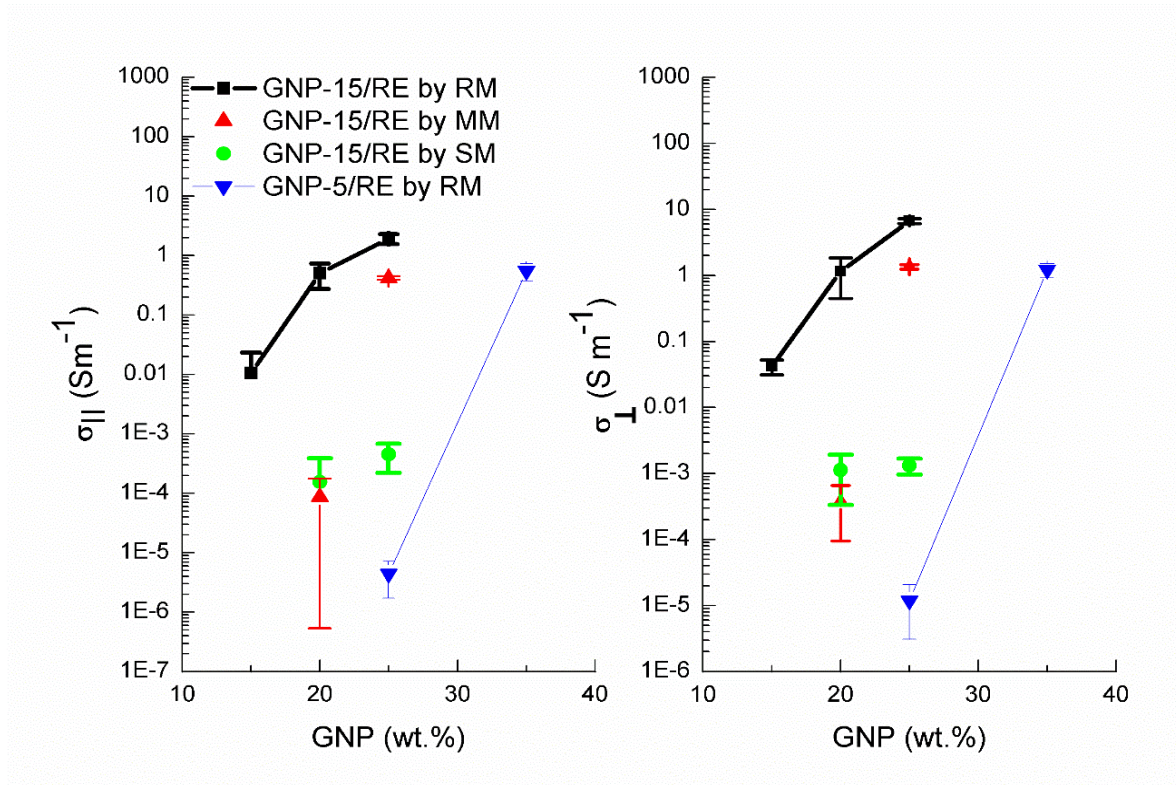


Fig. 8. Electrical conductivities of GNP-15/RE as a function of wt. % GNP-15s produced by RM, MM, and SM. Effects of platelet size is also presented. Errors are determined by measurements on 4-5 different specimens of each material.

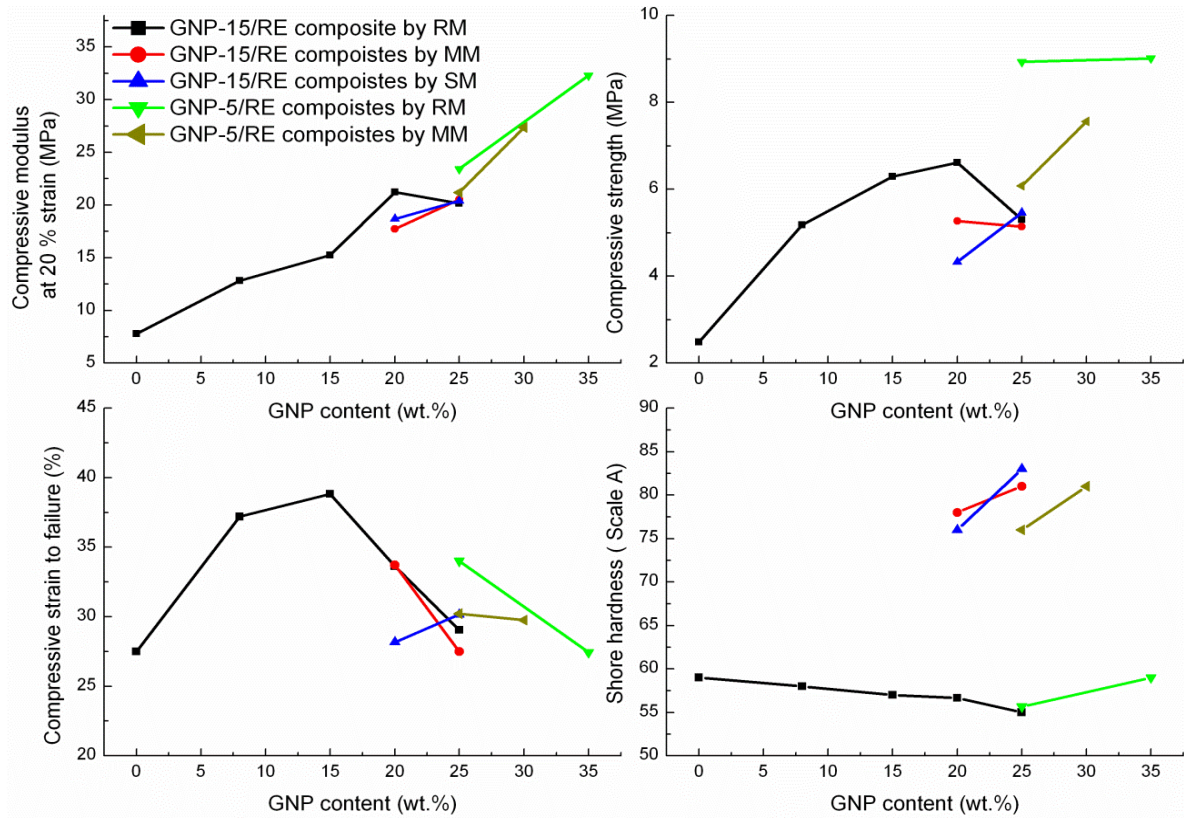


Fig. 9. Compressive properties and Shore hardnesses of GNP/RE composites as a function of wt. % of GNPs produced by RM, MM and SM. Data is averaged by testing 3-4 specimens of each material.

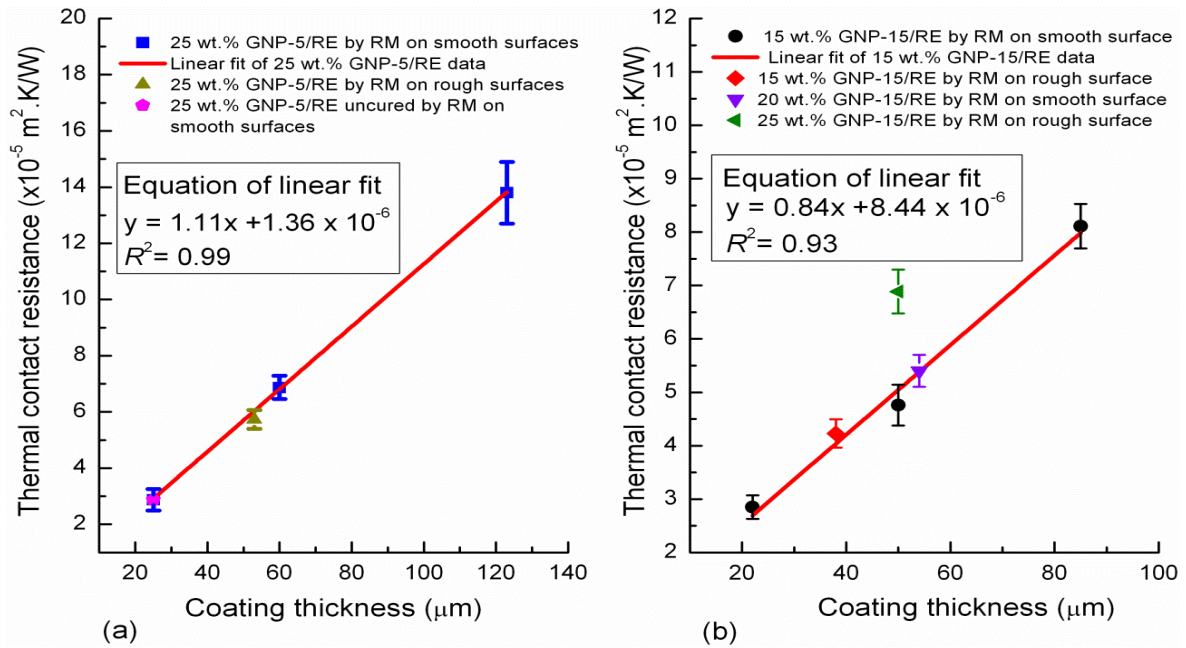


Fig. 10. Total thermal contact resistance vs. coating thickness of (a) 25 wt. % GNP-5/RE (RE) (b) 15 wt. % GNP-15/RE composite produced by RM measured on smooth and rough surfaces at 0.032 MPa compressive stress. The thermal contact resistance of 25 wt. % GNP-5/RE coating in an uncured state measured on smooth is also presented (a). The thermal contact resistance of 20 wt. % GNP-15/RE on smooth surface and 25 wt. % GNP-15/RE coating on rough surface is also presented (b). Linear fit and the equation of linear fit are also shown. Errors are obtained from at least 20 data points recorded under steady state conditions of 20-40 min.

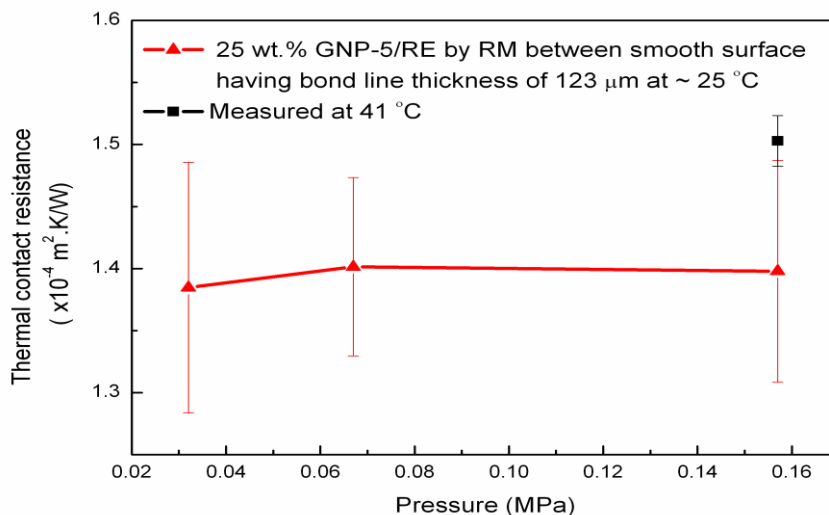


Fig. 11. Total thermal contact resistance of 25 wt. % GNP-5/RE between smooth surface as a function of applied pressure and temperature. Errors are obtained from at least 20 data points recorded under steady state conditions of 20-40 min.

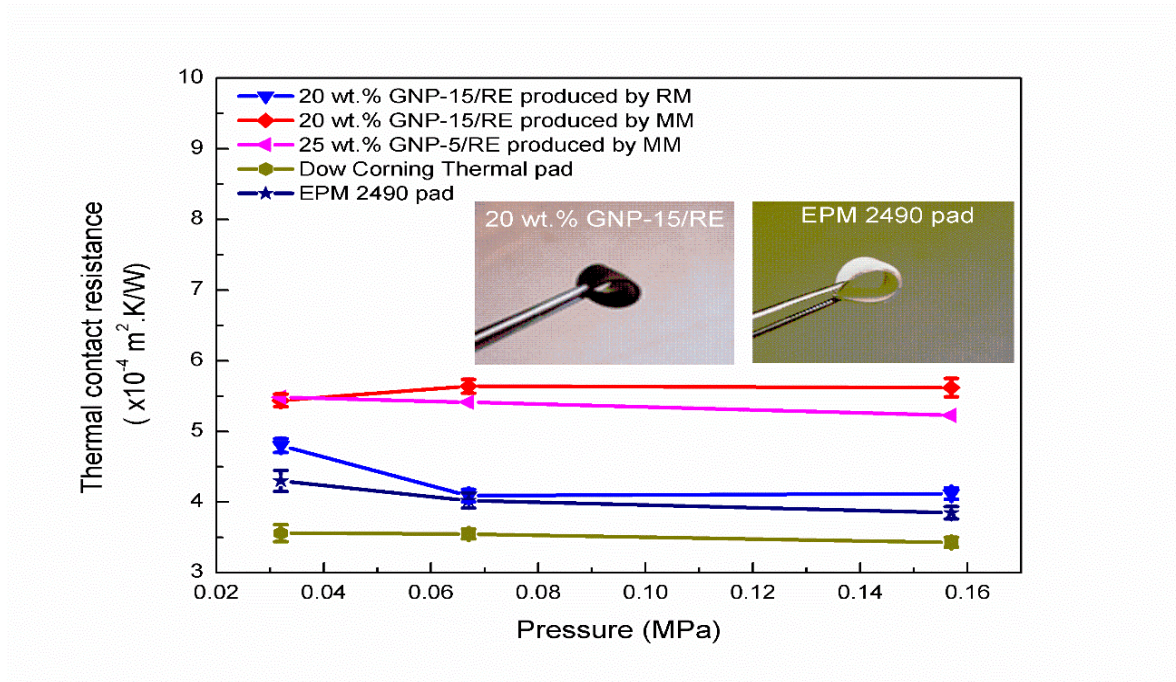


Fig. 12. Thermal contact resistance vs. applied pressure of GNP/RE and commercial pads measured at ~ 42 °C between smooth copper cylinders. Standard deviations are obtained from at least 20 data points obtained under steady state conditions of 20-40 min. Inset shows that 20 wt. % GNP-15/RE pad is easily foldable like commercial silicone (EPM 2490) thermal pad.